Journal of Applied Polymer Science

Mechanical and open hole tensile properties of self-reinforced PET composites with recycled PET fiber reinforcement

Chang-Mou Wu, Wen-You Lai
Department of Materials Science and Engineering, National Taiwan University of Science and Technology, Taipei, Taiwan 10607, Republic of China
Correspondence to: C.-M. Wu (E-mail: cmwu@mail.ntust.edu.tw)

ABSTRACT: The tensile strength of notched composites is an important factor for composite structural design. However, no literature is available on the notch sensitivity of self-reinforced polymer composites. In this study, self-reinforced recycled poly (ethylene terephthalate) (srrPET) composites were produced by film stacking from fabrics composed of double covered uncommingled yarns (DCUY). Composite specimens were subjected to uniaxial tensile, flexural, and Izod impact tests and the related results compared with earlier ones achieved on srPET composites reinforced with nonrecycled technical PET fibers. Effects of open circular holes on the tensile strength of srrPETs were studied at various width-to-hole diameter (W/D) ratios of the specimens. In the open hole tensile (OHT) measurements bilinear (yielding followed by post-yield hardening) stress–strain curves were recorded. The srrPET composites had extremely high yield strength retention (up to 142%) and high breaking strength retention (up to 81%) due to the superior ductile nature of the srrPETs, which induces plastic yielding near the hole thereby reducing the stress concentration effect. The results proved that srrPET composites are tough, ductile notch-insensitive materials. © 2016 Wiley Periodicals, Inc. J. Appl. Polym. Sci. **2016**, *133*, 43682.

KEYWORDS: composites; mechanical properties; polyesters; recycling

Received 8 December 2015; accepted 23 March 2016
DOI: 10.1002/app.43682

INTRODUCTION

The modern life style, supported by new production technologies, yields more and more polymeric waste materials creating severe disposal problems. Most of the polymer wastes are nondegradable and pollute the environment on long term. Accumulation of nonbiodegradable waste along with population growth is major factors of the environmental crisis all around the world.

Therefore, there is a growing interest for improved methods of recycling and reuse of polymeric composites. Efforts are also focused on the development of such polymer composites which can easily be reprocessed by melting. Self-reinforced polymer composites (srPCs, also termed to as single polymer composites or all-polymer composites) are excellent alternatives to traditional fiber-reinforced composites because both the reinforcing and the continuous phases involve polymers with the same chemical composition.[1–4] Numerous products, such as automotive components, luggage, sporting goods, and protective materials already use srPCs.

Various materials were used to prepare polyethylene,[5,6] polypropylene (PP),[7–9] polyethylene terephthalate (PET),[10–15] polymethyl methacrylate (PMMA),[16] liquid crystal copolymer,[17,18] polylactic acid (PLA),[19,20] and polyamide[21] based srPCs. There is a growing interest to produce value added products from PET waste. Development of new srPCs using recycled PET (rPET) fibers is fitting well into this "upcycling" strategy. Various fabrication methods such as hot compaction, overheating, co-extrusion, film stacking, and traditional melt or powder impregnation can produce srPCs. Hybrid or commingled yarns may also be suitable preforms of srPCs. They can be cost efficiently produced on existing industrial lines and easily converted in different textile architectures.[22,23] The cowrap spinning method has been successfully applied for developing srPETs.[24] In this study, rPET/copolymerized PET (mPET) commingled yarns were used to prepare srrPET composites and to evaluate their performance.

For the end applications of composite parts, drilling of holes is usually inevitable to provide access, or to facilitate joining.[25] Holes act as stress concentrators and thus disturb the stress distribution in the material. The tensile strength of notched composites is an important factor for composite structural design. Great numbers of authors have studied the effect of hole on the mechanical properties of composite structures. It has been

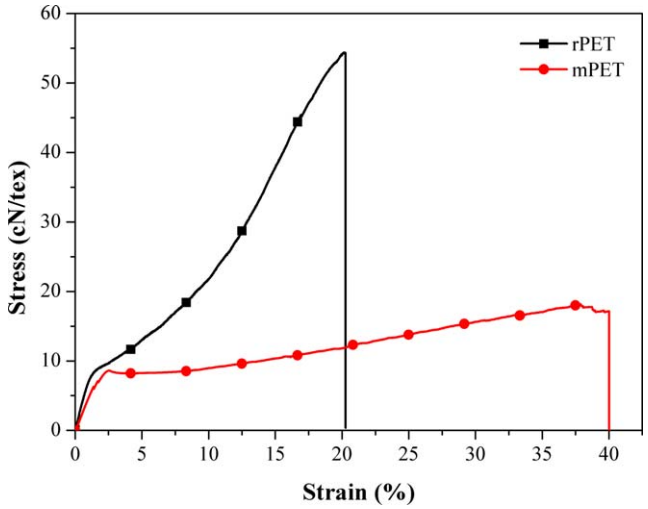

Figure 1. Tensile stress–strain curves of the rPET and mPET yarns. [Color figure can be viewed in the online issue, which is available at wileyonlinelibrary.com.]

shown[26–32] that the notched strength of composite laminates decreased with increasing notch size. Because of the stress concentration at the hole, as the load increases, damage initiates and propagates in the region around the hole, and support their early failure.

A material is ideally notch insensitive[27,31] (ideally ductile) if the failure stress is proportional to the net-sectional area, whereas it is ideally notch sensitive[28,29] (brittle) if it fails when the local stress at the edge of the hole equals the unnotched strength. The residual notch strength, i.e., the residual strength of a material in the presence of holes, is an important design parameter in engineering applications. A thermoplastic matrix provided better notched strength than a thermoset matrix in the corresponding composite due to its better toughness. The highly ductile behavior of thermoplastic-based laminates, at temperatures higher than their T_g, is very effective to accommodate overstresses near the hole. Mariatti *et al.*[27] reported that the highest strength reduction of ~75% was obtained in E-glass/ABS woven composites with a ratio of specimen width to hole diameter (W/D) of 3. The notch sensitivity of composites composed of metals and composite, termed as GLARE, was also assessed.[28] The presence of a hole in GLARE laminates gives a strength reduction about 40%. The combination of metals and composites results in a new family of hybrid laminates that have the ability to impede and arrest crack growth caused by cyclic loading, with excellent impact and damage tolerance characteristics and a low density. Many reports[28–30] are available on the open hole tensile of carbon and glass fiber reinforced thermoset-based composites which exhibiting moderate strength retention (~40–52%). Vieille *et al.*[30] investigated the notch effect of carbon fiber reinforced thermoplastic (polyphenylenesulfide or polyetheretherketone) composites, which exhibited a higher strength retention, viz. in the range of 50–58%. Several studies[31,32] confirmed that kenaf or flax/polypropylene composites exhibited outstanding strength retention (over 90%) owing to their superior ductility. By calculating the stress concentration factor, it was found that the kenaf/polypropylene nonwoven composites was relatively ductile and insensitive to the notch.[31] For woven fabric composites with holes, strain concentrations were generated by a combination of the stress concentration at the tip of the holes and the strain variation due to the different mechanical properties of woven fabric composites.[33] The stress concentration around the hole in a composite plate is a function of the material properties, specimen geometry and service loads. The stress concentration factor decreased with increasing hole diameters.[34]

Despite the recent developments with srPCs, no work is published on their notch sensitivity. To elucidate the effect of stress concentration on the tensile strength of srPET composites, specimens with open circular holes yielding various W/D ratios were tested in tension. Failure modes, damage initiation and the progression of notched srrPETs were also characterized and discussed.

EXPERIMENTAL

Materials

In this study, high tenacity recycled PET multifilaments (rPET), consisting of 111 tex multifilament bundles with a tenacity of 55.9 ± 2.2 cN/tex and strain of 20.6% ± 0.8% (Figure 1), were used as reinforcements. Every multifilament bundle consisted of 192 filaments. The copolymer PET yarn (mPET), composed of 35.6 tex multifilament bundles with a tenacity of 18.0 ± 1.1 cN/tex and strain of 36.1% ± 1.2% (Figure 1), was used as the matrix. Every multifilament mPET bundle consisted of 96 filaments. The DSC thermograms of the rPET and mPET yarns are shown in Figure 2. Two major melting peaks were found at 238 and 262 °C for the rPET yarns. In contrast, the melting temperature of mPET yarns is at 226 °C. The average viscosities of mPET measured at 238–250 °C were between 300 and 150 Pa s^{-1}. Conventional thermosetting processing methods are, therefore, not suitable for use with such highly viscous PET resins; thus, the method of film stacking was adapted for the fabric produced from the commingled yarns.

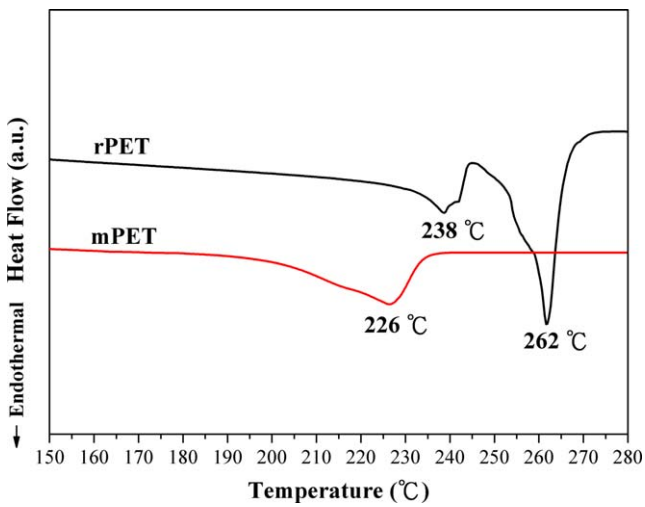

Figure 2. Thermograms of the rPET and mPET yarns. [Color figure can be viewed in the online issue, which is available at wileyonlinelibrary.com.]

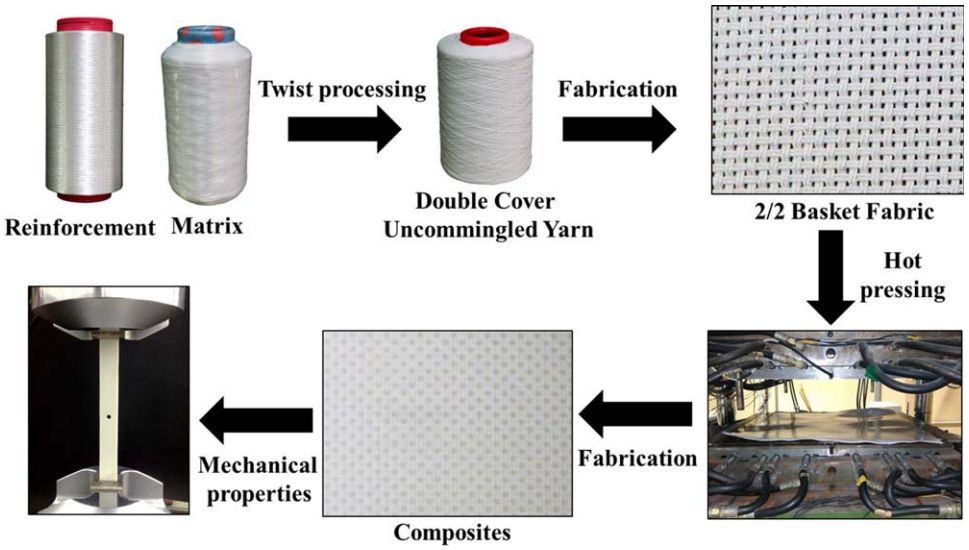

Figure 3. Flow chart of the srrPET sample preparation. [Color figure can be viewed in the online issue, which is available at wileyonlinelibrary.com.]

Sample Preparation

The flowchart for srrPET sample preparation is shown in Figure 3. The rPET and mPET multifilament yarns with a designed volume fraction of 53/47, were used to prepare the double covered uncommingled yarns (DCUYs) on a hollow spindle spinning machine. The high tenacity rPET multifilament yarn was used as reinforcing core yarn, and the mPET multifilament yarn was used as the wrapping material for the linear cowrap spinning yarns. The manufacture of DCUYs follows the same method in our previous articles.[24] The main spinning parameters are the number of turns (694 turns/m), machine rotation speed (5500 r.p.m.) and machine output (7.93 m min^{-1}). The DCUY was used as a feed material to produce 2/2 basket-woven fabric. The cowrap spinning yarns, which served as warp and weft yarns, were then woven on a rapier weave machine. The densities of the wrap and weft are 13.4 yarns/cm and 11.8 yarns/cm, respectively. In all the fabrics, the reinforcing fiber volume fraction was 53%.

srrPET composites were produced by a modified film stacking as described in our previous article.[24] Shrinkage problems may be encountered when heating dry fabrics and yarns. To reduce rPET fiber shrinkage and relaxation during heat consolidation processing, the fabric was first subjected to thermal setting for 3 min at 195 °C. The srrPET composites were fabricated with mass-production scale hot pressing system (FC-650TON, Long Chang, Taiwan). The srrPET composite sheet's dimension was 1 m^2. The manufacturing process is a very promising technology for the mass production of composites due to the reduction of cycle times. The srrPET composites were prepared by stacking five layers of fabric at 238 °C for 1 min under a pressure of 12 MPa. The thickness of srrPET composites is approximately 2 mm. It is worth noting that the difficulty of impregnation is largely improved owing to the good compatibility between the constituents in the srrPET composites. The fiber volume fraction and void content of srrPET composites are 53 and 1%, respectively.

Mechanical Tests

Tensile test of composites were performed by universal testing machine (MTS 810, MTS Systems Corporation, USA) with a load cell of 100 kN at room temperature according to the ASTM D3039 standard. Samples were prepared in dimension of 250 mm × 25 mm × 2 mm (length × width × thickness), and were clamped over an area of 50 × 25 mm^2 at each end, leaving a gauge length of 150 mm. Aluminum tabs were glued onto the ends of the specimens to create gripping areas. The grip pressure was hydraulically controlled. The testing crosshead speed was 5 mm min^{-1}. An average of five readings was taken for each sample.

Three point bending tests of the composites were performed on a universal testing machine, Trapezium X (AG-100 KNX, Shimadzu, Japan) according to the ASTM D790 standard. The dimension of specimens is 100 × 25 × 2 mm^3. A span length of 64 mm assured a span-to-depth ratio of 32, and crosshead speeds of 3.4 mm min^{-1} were adopted. An average of five readings was taken for each sample.

Izod impact test was performed at room temperature according to ASTM D256 standard on a pendulum impact tester (CPI, Atlas electric devices, USA) at impact energy of 5.5 J. The impact velocity was 3.4 m sec^{-1}. The dimension of the notched (2.7 ± 0.2 mm deep along the width) specimens was 63.5 ×

Table I. Tensile Properties of the srrPET Composites of Undrilled Specimen

Sample	Tensile strength (MPa)	Tensile strain (%)	Tensile modulus (GPa)	Yield strength (MPa)	Post-yield modulus (MPa)
srrPETs	121.3 ± 1.8	24.4 ± 0.7	3.4 ± 0.1	41.0 ± 1.3	323 ± 5
srPETs[24]	91.1 ± 9.0	23.4 ± 1.3	3.2± 0.2	22.3 ± 0.9	292 ± 30

Table II. Flexural and Impact Properties of the srrPET Composites

Sample	Flexural strength (MPa)	Flexural modulus (GPa)	Izod impact energy (J m^{-1})
srrPETs	82.0 ± 0.8	2.8 ± 0.3	1103 ± 64
srPETs[24]	77.9 ± 5.2	3.7 ± 0.2	710 ± 49

12.7 × 2 mm^3. The notches in the samples were opened by using a notch opener (QC-640, Cometech testing machines, Taiwan) for a notch tip radius of 0.25 mm. An average of five readings was taken for each sample.

Open hole tensile test of composites were performed by universal testing machine (MTS 810, MTS Systems Corporation, USA) with a load cell of 100 kN at room temperature according to the ASTM D5766 standard. The dimension of specimens was 250 mm × 25 mm × 2 mm. A drilling machine was used to make the open holes at the middle of the specimens equipped with aluminum end tabs. The circular holes were prepared through the center of the specimen using modified hollow-cylindrical steel drilling bits. The circular hole was machined by initially drilling a starter hole of small diameter, and then carefully enlarging it to the final dimensions by incremental drilling. To avoid delamination at the hole edge and to obtain a clean and smooth hole, a flat wooden plate was placed and clamped below the specimen. The notched region was hand polished using sand paper. Circular holes with three different diameters, namely 4, 6, and 8 mm, which were equivalent to W/D ratios of 6, 4, and 3 were studied for the open hole tensile test. The crosshead speed was 5 mm min^{-1}. An average of five readings was taken for each sample.

The gross nominal stress (σ_{gross}) is defined as

$$\sigma_{gross} = \frac{P}{W \times t} \quad (1)$$

where P is the load, W is the specimen width, and t is the specimen thickness.

The net nominal stress (σ_{net}) was calculated by the following equation:

$$\sigma_{net} = \frac{P}{(W-D) \times t} \quad (2)$$

Damaged specimens were inspected by stereo microscopy (S422L, Microtech, Taiwan) and scanning electron microscopy (SEM; JSM-6390LV, JEOL, Japan) to determine the failure modes. Prior to the SEM observations, the samples were mounted on aluminum stubs and sputter coated with a thin layer of gold to prevent electrical charging. SEM micrographs were taken using a 10 kV acceleration voltage at various magnifications.

RESULTS AND DISCUSSION

Tensile Properties of the srrPET Composites

The mechanical properties, including tensile strength, tensile modulus, tensile elongation, yield strength, and post-yield modulus are summarized in Table I. The tensile stress–strain curve shows a bilinear elastic-ductile behavior similar to that reported for srPETs in our previous studies.[24] Significant yielding and post-yield strain hardening were observed, which are indicative of the reinforcing effect and structural integrity of the srrPET composites. The tensile and yield strength of srrPETs are 121.3 and 41 MPa, respectively, which were 33 and 84% higher, respectively, than the values obtained for srPETs (Table I). This improvement may be attributed to better interfacial bonding caused by the partially fusing of the srrPET at the consolidation temperature, which facilitated the diffusion and entanglement between rPET and mPET molecules. The lower void content of srrPETs than srPET, caused by different manufacturing setup, may be another reason.

Flexural and Impact Properties of the srrPET Composites

Table II lists the flexural and impact properties of the srrPET composites. No significant difference was found in the flexural properties, impact strength and failure modes between the srrPET and srPET having the same reinforcing PET contents. The flexural strength and modulus of the srrPET composites are 82 MPa and 2.8 GPa, respectively. The lower flexural modulus in srrPETs was attributed to the lower tenacity of the rPET

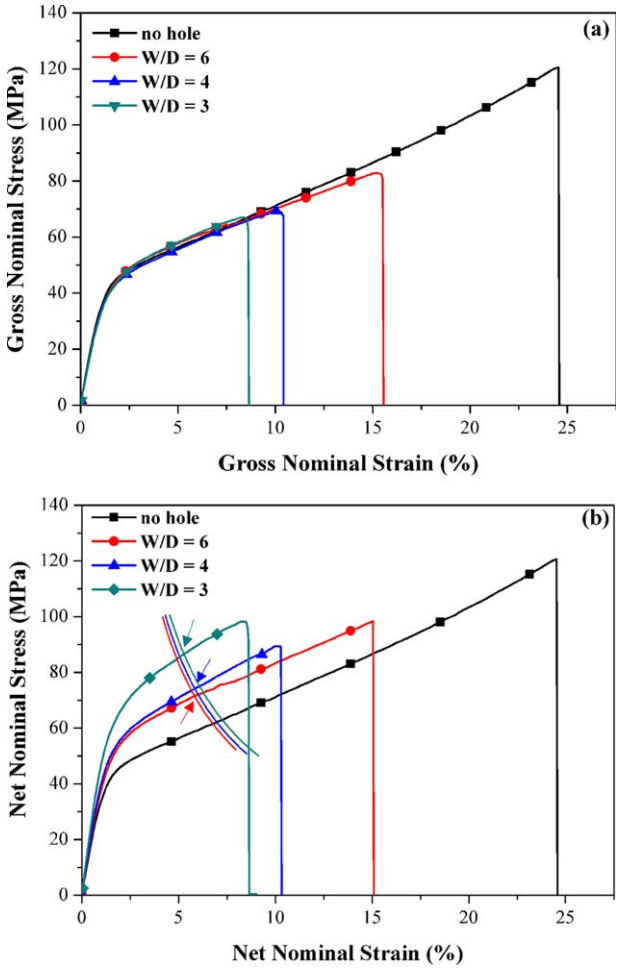

Figure 4. OHT properties of (a) gross nominal stress–strain curves and (b) net nominal stress-strain curves for srrPET composites with different *W/D* ratios. [Color figure can be viewed in the online issue, which is available at wileyonlinelibrary.com.]

Table III. Tensile Properties of the srrPET Composites of Undrilled and Open Hole Samples

Hole diameter (mm)	W/D	Strength (MPa)	Strain (%)	Modulus (GPa)	Yield strength (MPa)	Post-yield modulus (MPa)
0	N/A	121.3 ± 1.8	24.4 ± 0.7	3.4 ± 0.1	41.0 ± 1.3	322.5 ± 4.5
4	6	97.7 ± 1.5	14.4 ± 0.5	4.2 ± 0.1	48.3 ± 1.3	305.6 ± 14.4
6	4	89.9 ± 2.6	10.3 ± 0.2	4.4 ± 0.3	52.0 ± 2.1	394.6 ± 11.2
8	3	97.3 ± 0.7	7.9 ± 0.4	5.0 ± 0.1	58.2 ± 1.1	454.1 ± 17.8

fibers compared to the high tenacity of PET fibers used in srPET.

The Izod impact results (Table II) show high impact energy absorption (1103 J m^{-1}) in the srrPET composites compared to that of the srPETs (710 J m^{-1}). Unlike the full break apart failure of srPETs,[24] the impacted srrPET composites did not break apart most likely due to the use of low tenacity (and thus tougher) rPET fibers. Because of the plastic hinge effect, often observed for ductile polymer composites,[35] additional energy would be necessary to break the srPET composite sample. Accordingly, the real impact energy would be greater than the measured value.

Open Hole Tensile (OHT) Properties of the srrPET Composites

The open hole strength data may be useful for both materials' selection and for estimation of structural reliability. To elucidate the effect of stress concentration on the tensile strength of srrPET composites, specimens with open circular holes and different W/D ratios were tested with tension. The typical gross nominal stress–strain curves of srrPET composites with different W/D ratios are shown in Figure 4(a). A bilinear elastic-ductile behavior was found in the OHT srrPET composites. The gross nominal stress-strain curves of the open hole specimens followed the curve path of the undrilled reference specimen and showed earlier failure with increasing hole size. This demonstrates the structural integrity and notch insensitivity of srrPET composites. This unique OHT behavior has never been reported for fiber-reinforced composites. The typical net nominal stress-stain curves of srrPET composites are shown in Figure 4(b), and the OHT properties such as strength, strain, modulus, yield strength, and post-yield modulus at different W/D ratios are summarized in Table III. The OHT modulus, yield strength, and post-yield modulus increased with increasing hole size. The stiffening phenomenon results from the reduction in cross section area in open hole specimens at the same yield loading. When the specimens are loaded, the presence of holes causes the two ligaments to deform in the lateral direction. In this case, the inward contraction restrains the longitudinal deformation. Consequently, the longitudinal deformation of the affected region around the hole exhibits a smaller value. The result with the stiffening phenomenon has been observed by other researchers.[29] Yielding in the vicinity of the hole allows larger plastic deformation, which reduces the stress concentration, therefore, plastic deformation, rather than crack growth, occurred with increasing load prior to the rapid and unstable fracture. The tensile strength of the undrilled sample ($\sigma_{undrilled}$) is 121.3 MPa and that of the open hole samples are in the range of 90–98 MPa. The OHT strain (ε_{OHT}) decreased with increasing hole size from 24.4% (undrilled sample) to 7.9% ($W/D = 3$). The OHT strength (σ_{OHT}) results did not follow the trend of decreasing OHT strength with decreasing W/D ratio. The unusual results are attributed to the increased yield stress, which compensated for the decrease caused by strain reduction. Figure 5 shows how the hole size is changing before final failure as a function of sections of the net nominal stress-strain curve. For a larger hole size (8 mm), necking was clearly observed before fracture. The hole shape changed from circular to elliptical. The local strain at the hole edge was calculated according to the longitudinal deformation of the hole. A dramatic difference was observed between the OHT strain and the strain at the hole edge. A local strain of 60% was obtained at the ligament whereas the overall OHT strain was at 7.4%. This means an eight-fold increase. A local strain of 33% was obtained after the fracture of the specimens. This means a permanent deformation in the ligament area of the corresponding specimen and evidences the occurrence of stress concentration in open hole tensile loaded srrPET composites. Reasons for the high local deformation in the ligament area may be attributed to: (1) good interface bonding between the fiber and matrix thereby supporting the load transfer effectively, and preventing crack initiation and propagation. (2) Plastic yielding around the hole and resulting in efficient stress relief and redistribution.

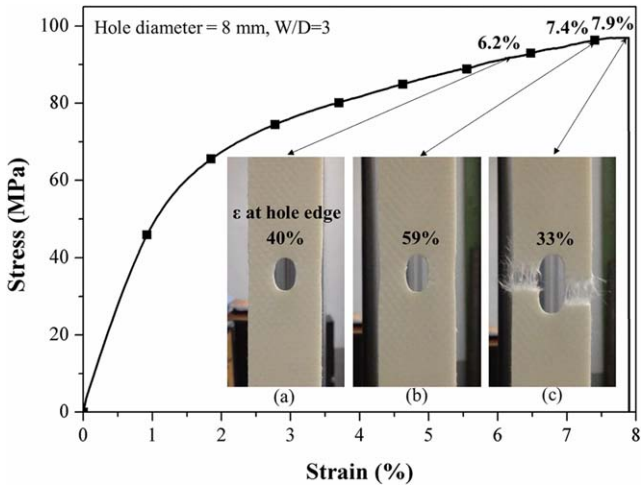

Figure 5. OHT behavior of srrPET composite with a W/D ratio of 3. Notes: this figure also shows macrophotographs taken at different net nominal strain values from the specimen. Strain at the hole edge (ligament) was calculated by the hole size in vertical. [Color figure can be viewed in the online issue, which is available at wileyonlinelibrary.com.]

Table IV. Comparison of Strength Retentions, Stress, and Strain Concentration Factors of srrPETs for Different W/D Ratios

W/D	Strength retention at yield (%)	Strength retention at break (%)	Theoretical stress concentration factor (K_t)	Effective stress concentration factor (K_σ)	Effective strain concentration factor (K_ε)
N/A	100	100	-	-	-
6	118	81	2.59	1.49	4.49
4	127	74	2.44	1.44	4.39
3	142	80	2.32	1.43	3.60

The notch strength retention is an important design parameter in engineering application, as emphasized before. The strength retention is used as a normalized value for comparing the tensile strengths of samples with different hole sizes, which have been calculated from the values of $\sigma_{\text{undrilled}}$ and σ_{OHT}. The strength retentions of srrPET for different *W*/*D* ratios are listed in Table IV. The strength retentions of srrPETs were 81, 74, and 80% with decreasing *W*/*D* ratio (i.e., = 6, 4, and 3), respectively. So, the strength retentions did not decrease with decreasing *W*/*D* but remained practically constant. As mentioned above, these unusual results were attributed to the increased yield stress that compensated for the stress decrease caused by strain reduction. Recall that bilinear elastic-ductile behavior with significant yielding was observed in srrPET composites. In practical structural design, the yield strength should be considered. Thus, the strength retentions at yield in srrPETs are also listed in Table IV. Such results were never discussed in the open literature according to the best knowledge of the authors due to the fact that yielding is a rare phenomenon in OHT tests of composites. The yield strength retentions of srrPET are 118, 127, and 142%, respectively, with decreasing *W*/*D* ratio. It is attributed to the superior ductile nature of the srrPETs, which induces plastic yielding near the hole thereby reducing the stress concentration effect. These results support our claim about the notch insensitivity of srrPET composites. Note that thermoset composites exhibited the lowest strength retentions—measured at break—(between 40 and 52%), followed by thermoplastic composites (between 43 and 81%). Some natural fiber reinforced thermoplastic composites exhibited, however, very high strength retentions (about 70 to 97%). Considering the above ranges, we can conclude that srrPETs is a highly ductile, notch-insensitive material. The highest stress occurring near the hole was mitigated by the nonlinear yielding behavior of srrPETs, especially for samples with the highest W/D ratio (=6 in our case).

To estimate the effects of the presence of holes on the carrying capacity of composite elements, it is highly desired to predict stress-strain concentrations at notches during the design of structures. Two quantities: the theoretical stress concentration factor (K_t) and the effective stress concentration factor (K_σ) are necessary to be considered and compared.

For the central single circular hole in finite-width plate ($0 \leq D/W \leq 1$), the theoretical (elastic) stress concentration factor (K_t) is defined as[36]

$$K_t = 3.00 - 3.13(D/W) + 3.66(D/W)^2 - 1.53(D/W)^3 \quad (3)$$

The K_t values of srrPETs for different *W*/*D* ratios were calculated and listed in Table IV. It was found that, as the W/D ratio decreased from 6 to 3 (increased the hole size), the K_t values decreased from 2.59 to 2.32.

For nonlinear materials, where local yield deformation can occur in the vicinity of the hole, Neuber's rule is probably the best-known approximate method for notch strain prediction. Neuber's rule allows a generalized consideration of elastic-plastic behavior for static uniaxial tension and is useful beyond the elastic limit relating the effective stress and strain concentration factors to the theoretical stress concentration factor. Neuber established that[36]:

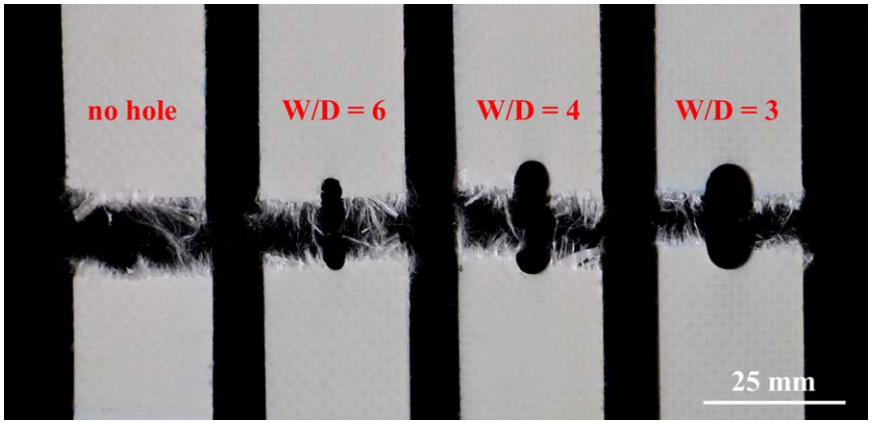

Figure 6. Optical images showing the final failure of OHT srrPET composites with different W/D ratios. [Color figure can be viewed in the online issue, which is available at wileyonlinelibrary.com.]

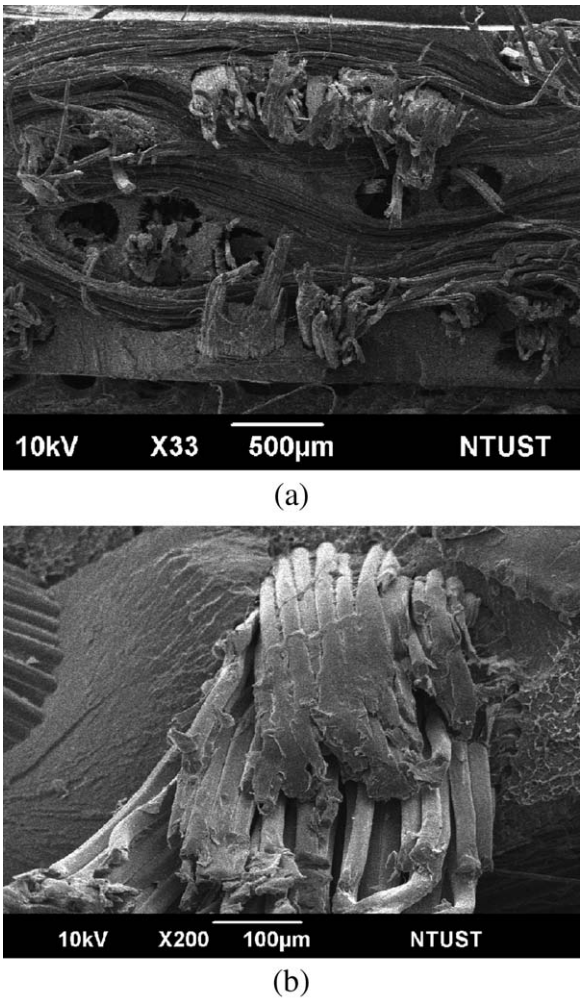

Figure 7. SEM image showing the (a) fracture surface and (b) cohesive failure for the OHT srrPET samples.

$$K_t^2 = K_\sigma K_\varepsilon \tag{4}$$

where

$$K_\sigma = \sigma_{max} / \sigma_{net} \tag{5}$$

$$K_\varepsilon = \varepsilon_{max} / \varepsilon_{net} \tag{6}$$

K_σ and K_ε are the effective stress concentration factor and effective strain concentration factor, respectively, where σ_{max} and ε_{max} are the maximum stress and strain in the vicinity of the hole, and σ_{net} and ε_{net} are the net nominal stress and strain in the remote field. The determination of ε_{net} is found from the material's stress-strain curves using the net nominal stress at yielding point.

Then Neuber's rule can also be written as[36]

$$\sigma_{max}\,\varepsilon_{max} = K_t^2 \sigma_{net} \varepsilon_{net} \tag{7}$$

In general, K_t, σ_{net} and ε_{net} are known for the material. Equation (7) is further written by

$$\sigma_{max}\,\varepsilon_{max} = C \tag{8}$$

where C is a known constant. Furthermore, solving eq. (8) simultaneously with the net nominal stress–strain curves [Figure 4(b)], the values of σ_{max} and ε_{max} were thus derived. The effective stress and strain concentration factors (K_σ and K_ε) were determined by using eqs. (5) and (6) and listed in Table IV.

The effective stress concentration factor K_σ values decreased with increasing hole size from 1.49 to 1.43, as indicated in Table IV. The theoretical factor was higher than the effective one: $K_t > K_\sigma$. The stress concentration for the smaller hole was much more localized than that for the larger one. For smaller hole size, where the hole edge looks like a sharp notch or crack and this leads to a higher stress. It is important to consider the failure of srrPETs in woven fabric structure. The srrPETs is a highly ductile material with nonlinear plastic yielding. The lower stress concentration factor was caused by the larger hole size and the superior ductile nature of the srrPETs, which induced localized plastic yielding near the hole. Similarly, the K_ε values decreased with increasing hole size from 4.49 to 3.60. The plastic yielding in the vicinity of the hole caused higher strain and thereby reducing the stress concentration effect.

Failure Mechanism

The OHT failures of srrPET specimens with different W/D ratios are shown in Figure 6; the specimens underwent break-apart failures. The specimens with different hole sizes exhibited similar failure modes before catastrophic failure. Fractography results, as shown in Figure 7(a), suggest that in the final fracture breakage and fiber pullout of warp yarns, splitting fracture of weft yarns, and resin fracture are involved. No delamination was observed in any of the srrPET composites with or without a hole. This may be ascribed to the good interfacial bonding [Figure 7(b)] and the nonplanar structure of woven fabric plies. As shown in Figure 7(a), fibers remaining within the pullout holes reveal good interfacial bonding between the fiber and matrix. Figure 8 illustrates the failure modes and mechanism of the OHT srrPET composites. Failure appears within fiber bundles and in the interlace points where the weft fibers undulate over warp fibers at the hole rim. It results in the splitting of the initially perpendicular weft and warp fibers bundles. This implies that the stress concentration was located at interlace points, which play a role to carry load and distribute the load to yarns in the warp and weft direction. The presence of yielding near the hole allows prominent plastic deformation, which reduces the stress concentration; therefore, plastic deformation, rather than crack growth, occurred with increasing load prior to fast and unstable catastrophic fracture. It is obvious that the

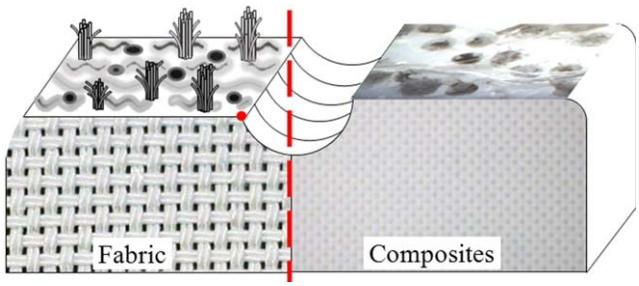

Figure 8. Failure modes of the OHT srrPET composites. [Color figure can be viewed in the online issue, which is available at wileyonlinelibrary.com.]

yield deformation, initiated at the hole edge and grew in size with increasing load up to the final fracture. The failure starts at the location of the highest yield deformation and grows perpendicular to the loading direction along the weft tows towards the edge of the specimen.

CONCLUSIONS

In this study high-quality srrPET composites were produced by using fabrics from double covered uncommingled yarns (DCUY) via a film stacking like method in hot pressing. The srrPET composites were subjected to uniaxial tensile, flexural, Izod impact and open hole tensile (OHT) tests. A bilinear elastic-ductile behavior was observed in the OHT srrPET composites tested in the W/D range of 3–6. The presence of yielding in the vicinity of the hole triggered plastic deformation, which reduced the stress concentration. And plastic deformation rather than crack growth occurred in the free ligament area upon increasing load prior to fast final fracture. Fractography results revealed that the latter was caused by breakage and fiber pullout of warp tows, splitting fracture of weft yarns, and resin fracture. No delamination was observed in all srrPET composites. The tensile strength of the undrilled sample was 121.3 MPa, and that of the open hole samples were in the range of 90–98 MPa. The OHT strain decreased with increasing hole size, from 24.4% (undrilled sample) to 7.9% ($W/D = 3$). The srrPET composites have extremely high yield strength retention up to 142% and high breaking strength retention up to 81%. The results reveal its superior ductile behavior and insensitive to the notch.

ACKNOWLEDGMENTS

Part of this work was financially supported by the Ministry of Science and Technology of Taiwan, ROC, under contract numbers: MOST 103-2622-E-011-017-CC3.

REFERENCES

1. Karger-Kocsis, J.; Bárány, T. *Compos. Sci. Technol.* **2014**, *92*, 77.
2. Fakirov, S. *Compos. Sci. Technol.* **2013**, *89*, 211.
3. Kmetty, Á.; Bárány, T.; Karger-Kocsis, J. *Prog. Polym. Sci.* **2010**, *35*, 1288.
4. Fakirov, S. *Macromol. Mater. Eng.* **2013**, *298*, 9.
5. Hine, P. J.; Olley, R. H.; Ward, I. M. *Compos. Sci. Technol.* **2008**, *68*, 1413.
6. Zhuang, X.; Yan, X. *Compos. Sci. Technol.* **2006**, *66*, 444.
7. Abraham, T.; Banik, K.; Karger-Kocsis, J. *eXPRESS Polym. Lett.* **2007**, *1*, 519.
8. Bárány, T.; Izer, A.; Karger-Kocsis, J. *Polym. Test.* **2009**, *28*, 176.
9. Abraham, T. N.; Wanjale, S. D.; Bárány, T.; Karger-Kocsis, J. *Compos. Part A* **2009**, *40*, 662.
10. Zhang, J. M.; Reynolds, C. T.; Peijs, T. *Compos. Part A* **2009**, *40*, 1747.
11. Zhang, J. M.; Peijs, T. *Compos. Part A* **2010**, *41*, 964.
12. Fakirov, S.; Duhovic, M.; Maitrot, P.; Bhattacharyya, D. *Macromol. Mater. Eng.* **2010**, *295*, 515.
13. Chen, J. C.; Wu, C. M.; Pu, F. C.; Chiu, C. C. *eXPRESS Polym. Lett.* **2011**, *5*, 228.
14. Wu, C. M.; Chang, C. Y.; Wang, C. C.; Lin, C. Y. *Polym. Compos.* **2012**, *33*, 245.
15. Schneider, C.; Kazemahvazi, S.; Åkermo, M.; Zenkert, D. *Polym. Test.* **2013**, *32*, 221.
16. Matabola, K.; De Vries, A.; Luyt, A.; Kumar, R. *eXPRESS Polym. Lett.* **2011**, *5*, 635.
17. Pegoretti, A.; Zanolli, A.; Migliaresi, C. *Compos. Sci. Technol.* **2006**, *66*, 1970.
18. Pegoretti, A.; Zanolli, A.; Migliaresi, C. *Compos. Sci. Technol.* **2006**, *66*, 1953.
19. Kimble, L. D.; Bhattacharyya, D.; Fakirov, S. *Express Polym. Lett.* **2015**, *9*, 300.
20. Gao, C.; Meng, L.; Yu, L.; Simon, G. P.; Liu, H.; Chen, L.; Petinakis, S. *Compos. Sci. Technol.* **2015**, *117*, 392.
21. Bhattacharyya, D.; Maitrot, P.; Fakirov, S. *eXPRESS Polym. Lett.* **2009**, *3*, 525.
22. Jiang, J.; Chen, N. *J. Compos. Mater.* **2012**, *46*, 2097.
23. Gobi Kannan, T.; Wu, C. M.; Cheng, K. B. *Compos. Part B* **2012**, *43*, 2836.
24. Wu, C. M.; Lin, P. C.; Tsai, C. T. *Polym. Compos.* Published online: 30 APR 2015, DOI: 10.1002/pc.23531.
25. Girão Coelho, A. M.; Mottram, J. T. *Mater. Des.* **2015**, *74*, 86.
26. Vieille, B.; Taleb, L. *Compos. Sci. Technol.* **2011**, *71*, 998.
27. Mariatti, M.; Nasir, M.; Ismail, H.; Backlund, J. *J. Reinf. Plast. Compos.* **2004**, *23*, 1173.
28. O'Higgins, R. M.; McCarthy, M. A.; McCarthy, C. T. *Compos. Sci. Technol.* **2008**, *68*, 2770.
29. Yudhanto, A.; Watanabe, N.; Iwahori, Y.; Hoshi, H. *Mater. Des.* **2012**, *35*, 563.
30. Vieille, B.; Aucher, J.; Taleb, L. *Mater. Des.* **2012**, *35*, 707.
31. Hao, A.; Yuan, L.; Chen, J. Y. *Compos. Part A* **2015**, *73*, 11.
32. Gobi Kannan, T.; Wu, C. M.; Cheng, K. B. *Compos. Part B* **2014**, *57*, 80.
33. Pandita, S. D.; Nishiyabu, K.; Verpoest, I. *Compos. Struct.* **2003**, *59*, 361.
34. Filippini, M. *Int. J. Fatigue* **2000**, *22*, 397.
35. Karger-Kocsis, J. *J. Appl. Polym. Sci.* **1992**, *45*, 1595.
36. Young, W. C.; Budynas, R. G. *Roark's Formulas for Stress and Strain*; New York: McGraw-Hill, **2002**; Vol. *7*, Chapter 17, p 771.